ISSN 1063-780X, Plasma Physics Reports, 2007, Vol. 33, No. 1, pp. 28–37. © Pleiades Publishing, Ltd., 2007.
Original Russian Text © T.M. Burinskaya, J.L. Rauch, 2007, published in Fizika Plazmy, 2007, Vol. 33, No. 1, pp. 32–42.

SPACE PLASMA

Waveguide Regime of Cyclotron Maser Instability in Plasma Regions of Depressed Density

T. M. Burinskaya[a] and J. L. Rauch[b]

[a] *Space Research Institute, Russian Academy of Sciences, Profsoyuznaya ul. 84/32, Moscow, 117997 Russia*
[b] *Laboratory of Physics and Chemistry of the Environment, National Center of Scientific Research, Orleans, France*

Received April 12, 2006; in final form, May 24, 2006

Abstract—The generation of auroral kilometric radiation from the Earth is studied in a waveguide model that describes the development of cyclotron maser instability in plasma regions of depressed density that have a finite length in one of the directions perpendicular to the magnetic field. A general dispersion relation for waves propagating in an arbitrary direction is derived. Numerical solutions to the dispersion relation show that the instability growth rate increases with wave vector component directed along a tangent to the source boundary in a plane perpendicular to the magnetic field. Waveguide eigenmodes are constructed, and it is shown that, in the general case, the electromagnetic field in the source has an asymmetric structure, the ratio of the electric field components in the source depends on the coordinates, and the electric field component transverse to the source boundary can substantially exceed the component parallel to the boundary. The results obtained are discussed from the standpoint of comparing them with satellite observational data.

PACS numbers: 52.35.Hr

DOI: 10.1134/S1063780X07010047

1. INTRODUCTION

Investigation of the cyclotron maser instability in plasma regions of finite length is of interest primarily because the experimental data obtained during the past decade have clearly shown that the sources of auroral kilometric radio emission are spatially bounded regions (cavities) in which the low-density hot plasma is very different from the surrounding, denser and cold, background plasma. Auroral kilometric radiation (AKR), which was first recorded by the *Electron-2* satellite in 1965 [1], is the most intense nonthermal natural emission from the Earth; its power can be as high as 10^7–10^9 W [2]. It has been established experimentally that AKR is generated in plasma regions of depressed density in which the electron Langmuir frequency is much lower than the electron gyrofrequency [3]. Wu and Lee [4] were the first to suggest that the source of AKR is electron cyclotron maser instability. At present, it is this instability that is thought to be the most probable physical mechanism responsible for the generation of the Earth's AKR and of similar types of radiation from the solar system's planets having their own magnetic field (Jupiter, Saturn, and Uranus). The sources of free energy that goes into the excitation of electromagnetic waves are hot electron fluxes from the Earth's magnetospheric tail into the auroral region. Time-resolved measurements performed by the *FAST* satellite showed that the electron distribution function in the AKR source has a "horseshoe" shape with $\partial f/\partial v_\perp > 0$, which results in efficient energy transfer from the electrons to the waves [5]. Until recently, the generation of AKR due to the development of cyclotron maser instability was investigated under the assumption that the plasma is homogeneous. However, an analysis of the experimental data from the *Viking* spacecraft showed that, in a plane perpendicular to the magnetic field, the length of the AKR generation region in one of the directions usually does not exceed 100 km, whereas the length in the latitudinal direction, as well as the length of the source along the magnetic field, is greater than 1000 km [6]. The width of the transition layer separating a denser cold background plasma from a low-density hot plasma of the AKR source is less than or on the order of the characteristic radiation wavelength. The electron energy in the source region is on the order of several keV, the energy of transverse motion of the electrons being much higher than their energy along the magnetic field. The cyclotron maser instability generates waves at frequencies close to the local electron gyrofrequency. Since the plasma density in the AKR source is lower than the density of the surrounding background plasma, the cutoff frequency of electromagnetic waves around the source is higher than the frequency of the excited waves. This is why the waves cannot immediately escape from the region where they were generated. The Earth's magnetic field decreases with altitude; therefore, for the waves to escape into the surrounding medium, they should propagate upward until their frequency becomes equal to the local cutoff frequency in the background plasma. The first waveguide model of the generation of AKR was developed by Louarn and Le Quéau [7]. They derived a dispersion relation and solved it numerically

for different source parameters. In what follows, however, it will be shown that the results obtained in [7] are valid only for waves whose wave vector component in the latitude direction is zero. We believe that the waveguide model of the generation of AKR holds considerable promise, especially in the light of recent experimental results. This motivated us to derive a dispersion relation that describes the generation of electromagnetic waves propagating in an arbitrary direction. We also present the results of numerically solving the dispersion relation for plasma parameters close to the experimentally observed ones and investigate how the spectral parameters of the AKR depend on the energy parameters of the electron plasma component in the source region. In the conclusion, we discuss our results in the context of comparing them with satellite observational data.

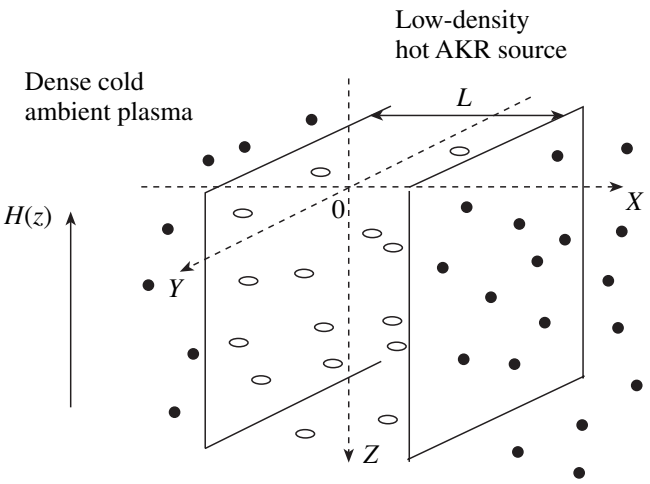

Fig. 1. Geometry of the AKR source model.

2. FORMULATION OF THE PROBLEM AND BASIC EQUATIONS

In order to investigate cyclotron maser instability in an auroral density cavity of finite dimensions, we use a model in which the AKR source is considered to be a plane waveguide that has the width $L = 2l$ along the x axis and is infinite in the y and z directions (see Fig. 1). The z axis is directed oppositely to the background magnetic field. The width of the transition layer between the low-density hot source plasma and the surrounding denser cold background plasma is assumed to be much less than the wavelength of the excited waves. The electron distribution in the waveguide is approximated by a ring function, $f(v_z, v_\perp) = (2\pi v_{\perp 0})^{-1}\delta(v_\perp - v_{\perp 0})\delta(v_z - v_0)$, where v_0 is the directed electron velocity along the magnetic field. That the use of such an idealized distribution function to investigate the generation of AKR is quite justified was shown in [8–10], where the results of calculations for a homogeneous plasma with a ring electron distribution were compared with those for more realistic distributions. The ions in our model are assumed to be immobile and to play the role of a neutralizing background.

Under the assumption that the plasma parameters vary on a characteristic spatial scale much greater than the source width, the plasma inside and outside the waveguide can be treated as homogeneous. We turn to Maxwell's equations for each of the three plasma regions, namely, the source region $-l \le x \le l$ and the surrounding background plasma regions $x > l$ and $x < -l$, with the corresponding dielectric tensor and apply the Fourier transformation in the y and z coordinates to them to write

$$\nabla \times \mathbf{H} = -i\frac{\omega}{c}(\hat{\varepsilon}\mathbf{E}), \quad \nabla \times \mathbf{E} = i\frac{\omega}{c}\mathbf{H}, \tag{1}$$

where c is the speed of light, $\hat{\varepsilon}$ is the dielectric tensor, and $\nabla = (\nabla_x, ik_y, ik_z)$. Substituting the ring function chosen for the electron distribution, $f(v_z, v_\perp) = (2\pi v_{\perp 0})^{-1}\delta(v_\perp - v_{\perp 0})\delta(v_z - v_0)$, into the expressions for the dielectric tensor elements [11] and taking into account the fact that, in the AKR generation region, the electron Langmuir frequency ω_p is much lower than the electron gyrofrequency ω_c and the characteristic wavelength of the excited waves is much larger than the electron gyroradius, we obtain

$$\begin{aligned} \varepsilon_{xx} &= \varepsilon_{yy} \equiv \varepsilon_1, \quad \varepsilon_{zz} = 1, \\ \varepsilon_{xy} &= -\varepsilon_{yx} \equiv \varepsilon_2, \quad \varepsilon_{xz} = \varepsilon_{yz} = \varepsilon_{zx} = \varepsilon_{zy} = 0. \end{aligned} \tag{2}$$

Here, $\varepsilon_1 = \varepsilon_1^i$ and $\varepsilon_2 = \varepsilon_2^i$ for the plasma in the AKR source region and $\varepsilon_1 = \varepsilon_1^0$ and $\varepsilon_2 = \varepsilon_2^0$ for the surrounding plasma, with

$$\begin{aligned} \varepsilon_1^i &= 1 - \frac{\alpha_i}{2\omega^2}(F_1 + F_2), \quad \varepsilon_2^i = \frac{\alpha_i}{2\omega^2}(F_1 - F_2), \\ F_1 &= \frac{\omega - N_z u_0}{\omega - 1 + \delta_\Sigma - N_z u_0} + \frac{v_\perp^2}{2c^2}\frac{N_z^2 - \omega}{(\omega - 1 + \delta_\Sigma - N_z u_0)^2}, \\ F_2 &= \frac{\omega - N_z u_0}{\omega + 1 - \delta_\Sigma - N_z u_0} + \frac{v_\perp^2}{2c^2}\frac{N_z^2 - \omega}{(\omega + 1 - \delta_\Sigma - N_z u_0)^2}, \\ \varepsilon_1^0 &= 1 - \frac{\alpha_0}{2\omega}\left(\frac{1}{\omega - 1} + \frac{1}{\omega + 1}\right), \\ \varepsilon_2^0 &= \frac{\alpha_0}{2\omega}\left(\frac{1}{\omega - 1} + \frac{1}{\omega + 1}\right). \end{aligned} \tag{3}$$

In relationships (3), we have introduced the dimensionless variables $\omega' = \omega/\omega_c$ (below, we will also introduce the dimensionless variable $\gamma' = \gamma/\omega_c$; for simplicity, the primes by the variables will be omitted), $N_z = k_z c/\omega_c$, $u_0 = v_0/c$, $\delta_\Sigma = (v_{\perp 0}^2 + v_0^2)/2c^2$, a $\alpha_i = \omega_{pi}^2/\omega_c^2$, and $\alpha_0 =$

ω_{p0}^2/ω_c^2. In the latter two variables, ω_{pi} and ω_{p0} are the electron plasma frequencies inside and outside the source, respectively. Using Eqs. (1) and relationships (2), we can express all the electromagnetic field components in terms of the longitudinal components of the electric and magnetic fields:

$$H_x = \frac{N_y E_z - N_z E_y}{\omega}, \quad H_y = \frac{i}{\omega}\frac{\partial E_z}{\partial x} + \frac{N_z}{\omega}E_x, \tag{4}$$

$$E_x = \frac{1}{D}\left\{ iN_z\left[\left(\varepsilon_1 - \frac{N_z^2}{\omega^2}\right)\frac{\partial E_z}{\partial x} + \varepsilon_2 N_y E_z\right] - \omega\left[\varepsilon_2\frac{\partial H_z}{\partial x} + N_y\left(\varepsilon_1 - \frac{N_z^2}{\omega^2}\right)H_z\right]\right\},$$

$$E_y = -\frac{1}{D}\left\{ N_z\left[\varepsilon_2\frac{\partial E_z}{\partial x} + \left(\varepsilon_1 - \frac{N_z^2}{\omega^2}\right)N_y E_z\right] + i\omega\left[-\left(\frac{N_z^2}{\omega^2} - \varepsilon_1\right)\frac{\partial H_z}{\partial x} + \varepsilon_2 N_y H_z\right]\right\}, \tag{5}$$

$$D = \omega^2\left[\left(\varepsilon_1 - \frac{N_z^2}{\omega^2}\right)^2 - \varepsilon_2^2\right],$$

where $N_y = k_y c/\omega_c$ and $x' = x\omega_c/c$. The longitudinal components E_z and H_z satisfy the dimensionless equations

$$\frac{1}{\omega^2}\frac{\partial^2 E_z}{\partial x^2} - \frac{N_y^2}{\omega^2}E_z + \left(1 - \frac{N_z^2}{\varepsilon_1\omega^2}\right)E_z = i\frac{N_z}{\omega}\frac{\varepsilon_2}{\varepsilon_1}H_z,$$
$$\frac{1}{\omega^2}\frac{\partial^2 H_z}{\partial x^2} - \frac{N_y^2}{\omega^2}H_z + \left(\frac{\varepsilon_1^2 - \varepsilon_2^2}{\varepsilon_1} - \frac{N_z^2}{\omega^2}\right)H_z = -i\frac{N_z}{\omega}\frac{\varepsilon_2}{\varepsilon_1}E_z, \tag{6}$$

which describe the propagation of an ordinary and an extraordinary wave. For strictly transverse propagation ($N_z = 0$), Eqs. (6) are independent of one another; the first of them describes an ordinary wave (O mode) and the second describes an extraordinary wave (X mode) with $N_\perp^2 = (N_x^2 + N_y^2) < 1$ ($\omega^2/\omega_c^2 \approx 1$).

In the general case, the solution to Eqs. (6) for the source region describes a superposition of two extraordinary and two ordinary waves. Accordingly, in the source region $-l \le x \le l$, the general solution has the form

$$H_z^i = (a_1\cos(N_1 x) + b_1\sin(N_1 x) + a_2\cos(N_2 x) + b_2\sin(N_2 x))\exp(i(N_y y + N_z z - \omega t)). \tag{7}$$

For the background plasma in the region $x > l$, the solution to Eqs. (6) can be written as

$$H_z^+ = (A_1\exp(iN_3(x - L/2)) + A_2\exp(iN_4(x - L/2)))\exp(i(N_y y + N_z z - \omega t)) \tag{8}$$

and, for the region $x < -l$, the solution has the form

$$H_z^- = (B_1\exp(-iN_3(x + L/2)) + B_2\exp(-iN_4(x + L/2)))\exp(i(N_y y + N_z z - \omega t)). \tag{9}$$

In expressions (7)–(9), N_1 and N_3 are transverse wavenumbers of the X mode inside and outside the source, respectively, and the transverse wavenumbers N_2 and N_4 refer to the O mode inside and outside the source. For each of the regions under analysis, the transverse wavenumbers are solutions to the dispersion relation in the case of a homogeneous plasma with the corresponding permittivity ε_1 or ε_2:

$$\left(1 - \frac{N_z^2}{\varepsilon_1\omega^2} - \frac{N_\perp^2}{\omega^2}\right)\left(\frac{\varepsilon_1^2 - \varepsilon_2^2}{\varepsilon_1} - \frac{N_z^2 + N_\perp^2}{\omega^2}\right) = \frac{N_z^2\varepsilon_2^2}{\omega^2\varepsilon_1^2}. \tag{10}$$

In the general case, the dispersion relation for determining the eigenmodes of the waveguide are found from the continuity conditions for the electromagnetic field components H_z, E_z, H_y, and E_y at the boundaries of the waveguide region.

3. ANALYSIS OF THE DISPERSION RELATION

3.1. Eigenmodes with $N_z = 0$

The X mode ($E_z = 0$) and O mode ($H_z = 0$) propagating perpendicular to the magnetic field are independent of one another. Therefore, in this case, only the terms describing the X mode should be taken into account in general solution (7)–(9); i.e., we must set $a_2 = b_2 = A_2 = B_2 = 0$. Substituting solution (7)–(9) into expression (5) and using the boundary conditions $H_z^i = H_z^+$ and $E_y^i = E_y^+$ at $x = l$ and $H_z^i = H_z^-$, and $E_y^i = E_y^-$ at $x = -l$, we arrive at the set of four equations

$$a_1\cos(N_1 l) + b_1\sin(N_1 l) = A_1,$$
$$a_1\cos(N_1 l) - b_1\sin(N_1 l) = B_1,$$
$$\frac{1}{D^i}\{a_1[\varepsilon_1^i N_1\sin(N_1 l) - \varepsilon_2^i N_y\cos(N_1 l)] - b_1[\varepsilon_1^i N_1\cos(N_1 l) + \varepsilon_2^i N_y\sin(N_1 l)]\} = -\frac{A_1}{D^0}[iN_3\varepsilon_1^0 + \varepsilon_2^0 N_y], \tag{11}$$
$$\frac{1}{D^i}\{a_1[\varepsilon_1^i N_1\sin(N_1 l) + \varepsilon_2^i N_y\cos(N_1 l)]$$

$$+ b_1[\varepsilon_1^i N_1 \cos(N_1 l) - \varepsilon_2^i N_y \sin(N_1 l)]\}$$
$$= -\frac{B_1}{D^0}[iN_3\varepsilon_1^0 - \varepsilon_2^0 N_y],$$

where D^i is given by expression (5) with ε_1^i and ε_2^i and D^0 is given by the same expression but with ε_1^0 and ε_2^0. The condition for Eqs. (11) to be consistent with one another yields the dispersion relation

$$\left\{\frac{1}{D^i}[\varepsilon_1^i N_1 \sin(N_1 l) - \varepsilon_2^i N_y \cos(N_1 l)] + \frac{\cos(N_1 l)}{D^0}[iN_3\varepsilon_1^0 + \varepsilon_2^0 N_y]\right\}$$
$$\times\left\{\frac{1}{D^i}[\varepsilon_1^i N_1 \cos(N_1 l) - \varepsilon_2^i N_y \sin(N_1 l)] - \frac{\sin(N_1 l)}{D^0}[iN_3\varepsilon_1^0 - \varepsilon_2^0 N_y]\right\}$$
$$= -\left\{\frac{1}{D^i}[\varepsilon_1^i N_1 \sin(N_1 l) + \varepsilon_2^i N_y \cos(N_1 l)] + \frac{\cos(N_1 l)}{D^0}[iN_3\varepsilon_1^0 - \varepsilon_2^0 N_y]\right\}$$
$$\times\left\{\frac{1}{D^i}[\varepsilon_1^i N_1 \cos(N_1 l) + \varepsilon_2^i N_y \sin(N_1 l)] - \frac{\sin(N_1 l)}{D^0}[iN_3\varepsilon_1^0 + \varepsilon_2 N_y]\right\}. \quad (12)$$

Note that dispersion relation (12) depends on N_y^2, as it should be, because there is no difference between waves propagating in the positive or negative direction of the y axis. In [7], cyclotron maser instability was investigated using a model identical to that adopted here. However, the dispersion relation obtained in [7] depends on N_y; therefore, it is valid only for $N_y = 0$.

The solutions to dispersion relation (12) with $N_y = 0$ constitute a discrete family of waveguide eigenmodes, each of which can be assigned an integer n. In our analysis, we define this integer as $n \approx 1 + N_1 L/\pi$ (where $L = 2l\omega_c/c$), i.e., as the number of maxima of the function $|H_z|$.

For each n value, the real and imaginary parts of the wave frequency as functions of N_y were found by numerically solving dispersion relation (12). In what follows, we will present the results calculated for the parameter values $\alpha_i = 0.002$, $\alpha_0 = 0.01$, $\delta_\Sigma = 0.0075$, and $l = \omega_c l/c = 60$, which are typical of AKR generation regions [6]. These parameter values are such that, at altitudes with the electron gyrofrequency $f_c \approx 200$ kHz, the source width is ~30 km; the electron density and energy inside the source are ~1 cm^{-3} and ~4 keV, respectively; and the background plasma density outside the source is ~5 cm^{-3}. In this section, we set $u_0 = 0$, because, according to experimental data, the energy of the directed motion of the electrons is much lower than their thermal energy. The role of the directed electron motion ($u_0 \neq 0$) will be discussed below. The results of solving dispersion relation (12) numerically for a family of eigenmodes with the numbers n are presented in Fig. 2 as the dependence of the normalized wave frequency $\delta\omega = (\omega - \omega_c)/\omega_c$ on the y component of the wave vector, $N_y = k_y c/\omega_c$ (Fig. 2a) and the dependence of the instability growth rate normalized to the electron gyrofrequency on the same wave vector component N_y (Fig. 2b).

Numerical simulations show that the higher the number n of the eigenmode, the narrower the range of N_y values at which the waves can be amplified ($\gamma > 0$). This stems from the facts that the higher the number n of the eigenmode, the larger the transverse wavenumber N_1 corresponding to it, $n \approx 1 + N_1 L/\pi$, and that the refractive index for the X mode should be less than unity, $N_1^2 + N_y^2 < 1$. Therefore, for each eigenmode with the number n, there is a limiting value of N_y, or, in other words, short-wavelength modes cannot propagate at small angles to the y axis. For essentially all of the eigenmodes, the growth rate is not a monotonically decreasing function of the y component of the wave vector, N_y, the only exception being short-wavelength modes with large numbers n. Instead, the growth rate is maximum at the limiting value of N_y for a given mode, so the eigenmodes of the waveguide propagate at the smallest possible angles to the y axis. In this case, the maximum growth rate increases with decreasing the mode number n. The calculations illustrated in Fig. 2 were carried out for $l = 60$. The results presented in Fig. 3 in the form of the dependence of $\delta\omega$ and γ on N_y for the $n = 12$ mode were obtained for the same plasma parameters as in Fig. 2, specifically, $\alpha_i = 0.002$, $\alpha_0 = 0.01$, and $\delta_\Sigma = 0.0075$, but for different widths of the source: $l = 30$ (dashed curves), 60 (dotted curves), and 120 (solid curves). As was expected, the smaller the width of the source, the slower the maximum growth rate and the narrower the range of N_y values in which the waves can be amplified. The latter circumstance is attributed to the fact that the transverse wavenumber N_1 corresponding to a mode with a fixed number n (in the case at hand, this is $n = 12$ mode) increases with decreasing source width, $N_1 \approx \pi((n-1)/L)$.

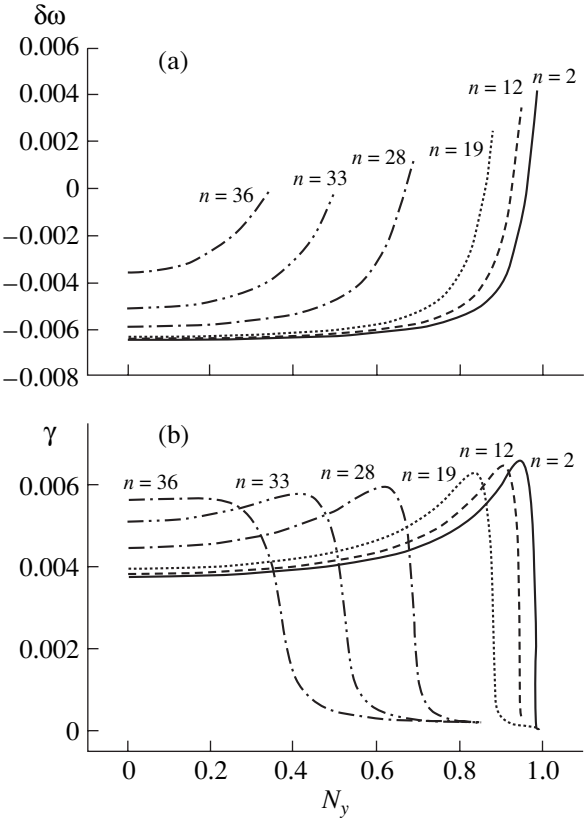

Fig. 2. (a) Normalized wave frequency δω and (b) instability growth rate γ as functions of N_y for several waveguide eigenmodes with the numbers n.

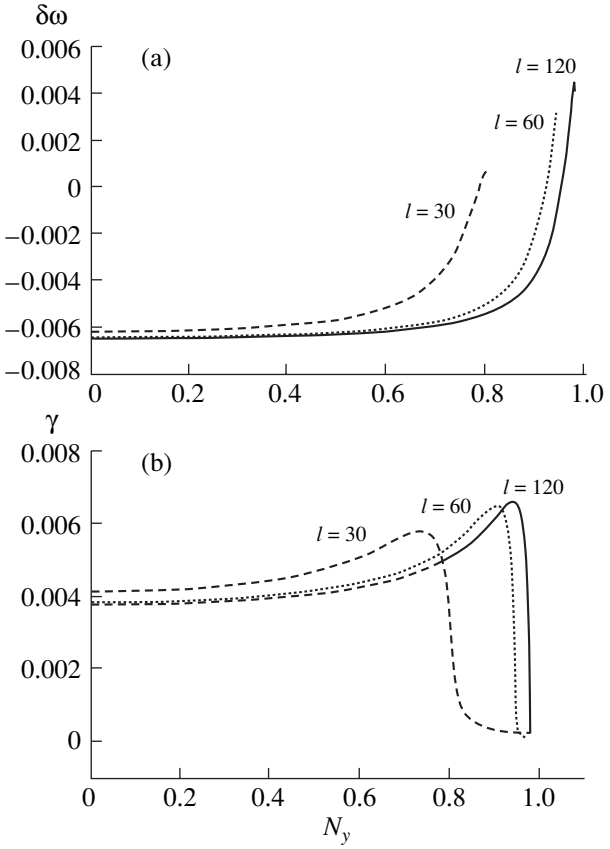

Fig. 3. (a) Normalized wave frequency δω and (b) instability growth rate γ as functions of N_y for the $n = 12$ eigenmode at different values of l.

It is of interest to compare the solutions to dispersion relation (12) with those to the dispersion relation for a homogeneous plasma. Since, in a homogeneous plasma, there is no preferred direction for waves in a plane perpendicular to the magnetic field, in Fig. 4 we show the dependence of the growth rate on $N_\perp = \sqrt{N_1^2 + N_y^2}$ for two different values of the electron energy in the source region, the values of the remaining plasma parameters being the same. The curves of group a were calculated for $\delta_\Sigma = 0.0125$, while the curves of group b were calculated for $\delta_\Sigma = 0.0075$. Each group shows solutions to dispersion relation (12) for the $n = 12$ mode at different values of l, namely, $l = 30$, 60, and 120, which refer to the dashed, dotted, and solid curves (like in Fig. 3). The plasma densities inside and outside the source are the same as those in Figs. 2 and 3. Hence, curves b in Fig. 4 are identical to the curves in Fig. 3b. The dispersion relation for a homogeneous plasma was solved under the assumption that the plasma density is the same over the entire region under consideration and is equal to that inside the source. The numerical results show that the growth rates calculated for a homogeneous plasma coincide with those obtained for a finite-size AKR source of width $l = 120$. In Fig. 4, the solid curves show the dependences $\gamma(N_\perp)$ for a source of width $l = 120$ and for a homogeneous plasma. Hence, for the above plasma parameters, we can see that, even in a source with a width on the order of 60 km, the linear instability growth rate is the same as that in a homogeneous plasma. The main effect of the finite width of the source is that there is a preferred propagation direction in which the waves grow at the fastest rate, specifically, the propagation direction that makes almost the smallest angle with the y axis.

It can be seen from Fig. 4 that the higher the energy of the transverse electron motion, the faster the growth rate and the wider the frequency range in which the waves can be generated. Figure 5 shows the dependence $\delta\omega(\gamma)$ for the $n = 12$ eigenmode in a source with the half-width $l = 60$, calculated for $\delta_\Sigma = 0.0125$ (dashed curve), 0.01 (dotted curve), and 0.0075 (solid curve), the parameter values $\alpha_i = 0.002$ and $\alpha_0 = 0.01$ being the same as in Fig. 4. It is easy to see that, as δ_Σ increases, the instability range expands to lower frequencies and the bulk of the waves excited during the development of cyclotron maser instability have frequencies far below the cutoff frequency in the background plasma. Consequently, at large values of δ_Σ, the waves grow in amplitude not only at the expense of the fast growth rates but

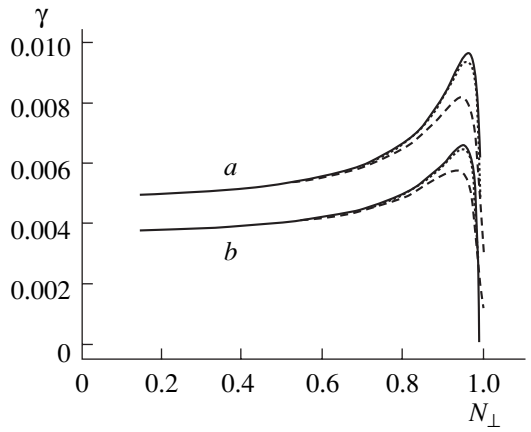

Fig. 4. Comparison of the calculated dependence $\gamma(N_\perp)$ for a homogeneous plasma at δ_Σ = (*a*) 0.0125 and (*b*) 0.0075 with calculations for sources of finite sizes (see text for details).

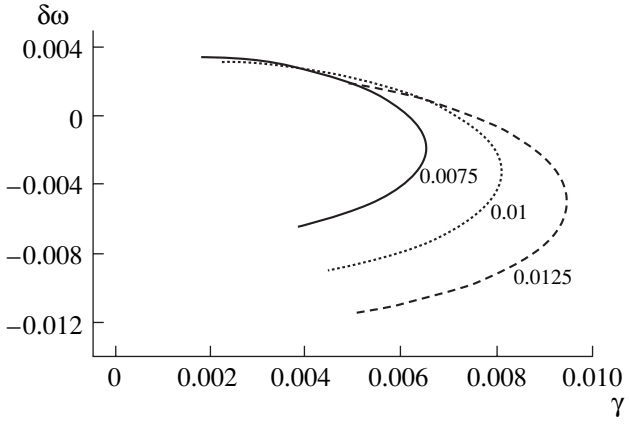

Fig. 5. Normalized wave frequency δω of the $n = 12$ eigenmode vs. γ for $l = 60$, $\alpha_i = 0.002$, $\alpha_0 = 0.01$, and different values of δ_Σ.

also because they can remain within the source (waveguide) region for a longer time.

Figure 6 shows solutions calculated for $\delta_\Sigma = 0.0075$ and for different densities of a homogeneous plasma. We can see that, for $\omega_p < 0.1\omega_c$ ($\alpha_i < 0.01$), the growth rate is maximum at an $N_\perp$ value close to unity. For higher densities ($\alpha_i > 0.01$), the growth rate is a monotonically decreasing function of the transverse wavenumber $N_\perp$; however, the range of $N_\perp$ values in which extraordinary waves can be generated narrows sharply as the density increases. For $\alpha_i > 0.03$, the waves in the system cease to be generated.

For comparison, Fig. 7 shows solutions to dispersion relation (12) for the $n = 12$ eigenmode, calculated for different plasma densities in the source. Curves *a* were obtained for $\alpha_i = 0.01$, while curves *b*, for $\alpha_i = 0.002$. The background plasma density outside the source is $\alpha_0 = 0.01$, and the electron energy is such that $\delta_\Sigma = 0.0075$. The dependence $\gamma(N_\perp)$ was calculated for $l = 30$ (dashed curves), 60 (dotted curves), and 120 (solid curves), as in Fig. 3. The solutions obtained for $l = 120$ coincide with those for a homogeneous plasma. An interesting point to note is that, according to numerical calculations, a quasi-waveguide solution (7)–(9) can exist for the same plasma densities inside and outside the source, $\alpha_i = \alpha_0$, provided that there are sufficiently many high-energy electrons in the source region.

3.2. Structure and Polarization of the Eigenmodes

The ratio of the coefficients $\frac{b_1}{a_1}$ in expression (7) determines the shape of the profile of $|H_z|$ along the *x* axis in the source. This ratio is found from the set of Eqs. (11) and has the form

$$\frac{b_1}{a_1} = \frac{\left\{\frac{1}{D^i}[\varepsilon_1^i N_1 \sin(N_1 l) - \varepsilon_2^i N_y \cos(N_1 l)] + \frac{\cos(N_1 l)}{D^0}[iN_3\varepsilon_1^0 + \varepsilon_2^0 N_y]\right\}}{\left\{\frac{1}{D^i}[\varepsilon_1^i N_1 \cos(N_1 l) + \varepsilon_2^i N_y \sin(N_1 l)] - \frac{\sin(N_1 l)}{D^0}[iN_3\varepsilon_1^0 + \varepsilon_2 N_y]\right\}}. \quad (13)$$

Using relationship (13), we can graphically illustrate how the structure of the eigenmode changes with varying N_y (at $N_z = 0$). Figure 8 displays the structure of the function $|H_z|$ in dimensionless units for the $n = 12$ eigenmode, calculated for the plasma parameters $\alpha_i = 0.002$, $\alpha_0 = 0.01$, $\delta_\Sigma = 0.0075$, and $l = 60$, for which we have $N_1 = 0.289$. The symmetric solution (Fig. 8a) corresponds to the eigenmode with $N_y = 0$, while the asymmetric solution (Fig. 8b), to the eigenmode with $N_y = 0.5$.

For $N_y = 0$, the polarization of the X mode is independent of the *x* coordinate in the source and the ratio $|E_x|/|E_y|$ is constant, $|E_x|/|E_y| = \varepsilon_2/\varepsilon_1 < 1$. Hence, for $N_y = 0$, the electromagnetic field is dominated by the E_y component. However, as the *y* component of the wave vector increases, the polarization becomes coordinate-dependent and the ratio $|E_x|/|E_y|$ can be much greater

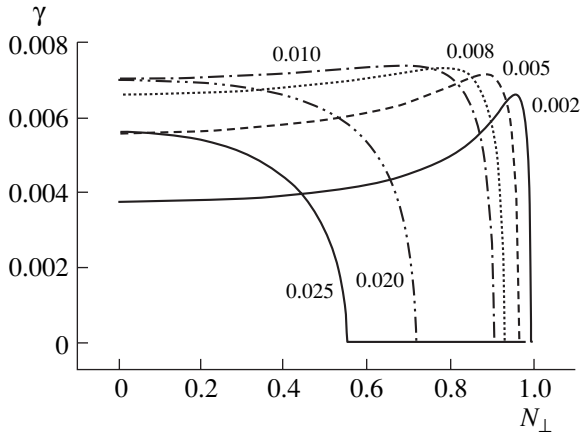

Fig. 6. Dependence $\gamma(N_\perp)$ for a homogeneous plasma at different values of $\alpha_i = (\omega_p/\omega_c)^2$.

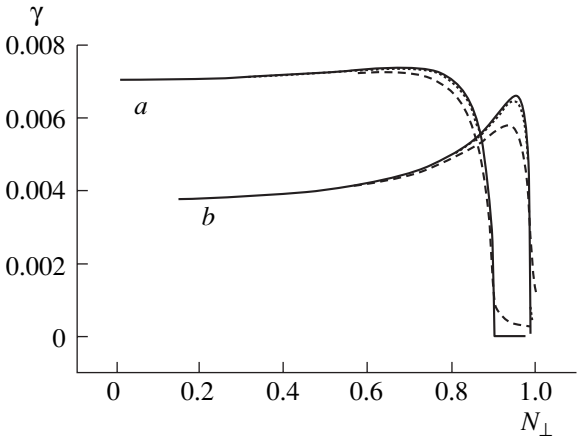

Fig. 7. Dependence $\gamma(N_\perp)$ for the $n = 12$ eigenmode at different values of the ratio ω_p/ω_c.

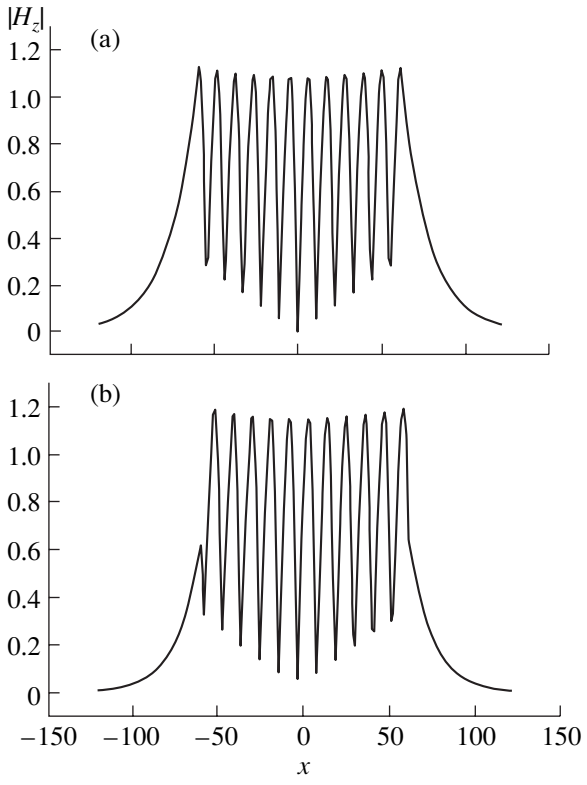

Fig. 8. Dependence $|H_z|(x)$ for the $n = 12$ eigenmode ($l = 60$) with different values of N_y: N_y = (a) 0 and (b) 0.5.

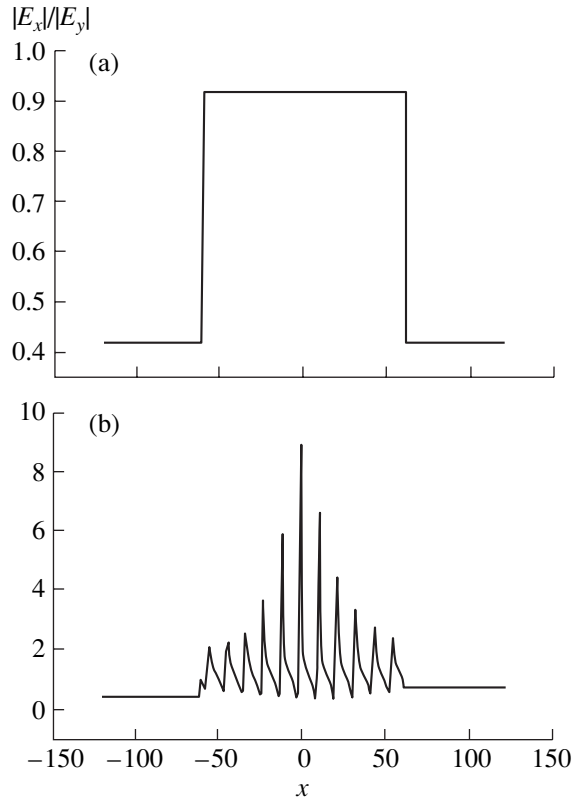

Fig. 9. Ratio of the absolute values of the electric field components, $|E_x|/|E_y|$, vs. x coordinate for the $n = 12$ eigenmode ($l = 60$) with different values of N_y: N_y = (a) 0 and (b) 0.5.

than unity. Figure 9 depicts the ratio $|E_x|/|E_y|$ as a function of the x coordinate for the eigenmodes shown in Fig. 8. We can clearly see that, for asymmetric solutions, the structure of the polarization of the waves within the source differs radically from that for symmetric solutions.

3.3. Eigenmodes of Electromagnetic Waves Propagating at an Arbitrary Angle to the Magnetic Field

The dispersion relation for electromagnetic waves propagating at an arbitrary angle to the external magnetic field is derived in the waveguide approximation

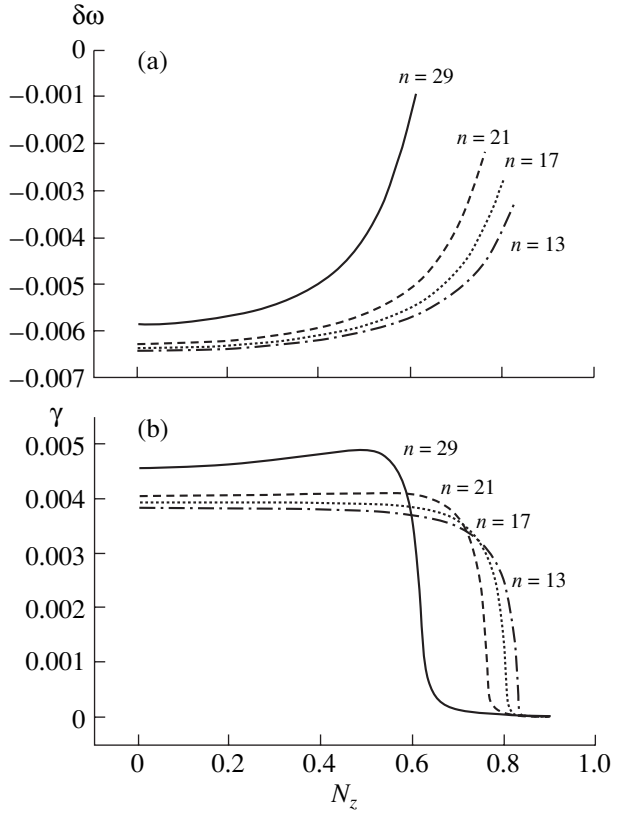

Fig. 10. (a) Normalized wave frequency δω and (b) instability growth rate γ as functions of N_z for several waveguide eigenmodes with the numbers n and with $N_y = 0$.

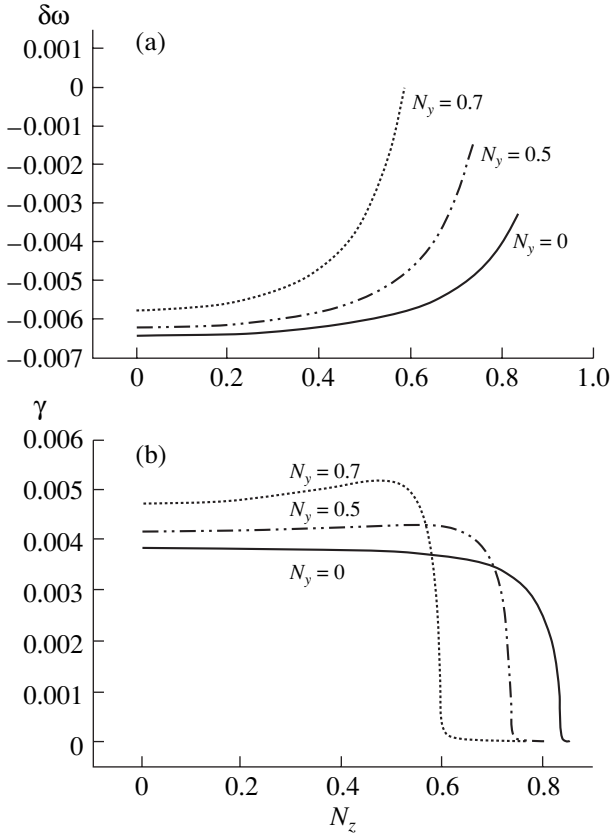

Fig. 11. (a) Normalized wave frequency δω and (b) instability growth rate γ as functions of N_z for the $n = 12$ eigenmode with different values of N_y.

from general solutions (7)–(9) and the boundary conditions $H_z^i = H_z^+$, and $E_y^i = E_y^+$ at $x = l$ and $H_z^i = H_z^-$, and $E_y^i = E_y^-$ at $x = -l$. Since this dispersion relation is extremely involved, we do not write it out here in explicit form and restrict ourselves to discussing some results of its numerical solution.

Figure 10 shows how the normalized frequency δω and growth rate γ depend on the wavenumber $N_z = k_z c/\omega_c$ for several eigenmodes with the numbers n and with $N_y = 0$. The calculations were carried out for the same values of the plasma parameters as those in Fig. 2, namely, $\alpha_i = 0.002$, $\alpha_0 = 0.01$, $\delta_\Sigma = 0.0075$, and $l = 60$. We clearly see that, as expected, the higher the number n of the eigenmode, the narrower the range of wavenumbers N_z in which the waves can be generated ($\gamma > 0$).

However, in contrast to Fig. 2, which shows an analogous dependence of the frequency and growth rate on N_y for the case of strictly transverse propagation ($N_z = 0$), the growth rate in Fig. 10b increases with the number n of the eigenmode. The behavior of the normalized frequencies and growth rates of the $n = 12$ eigenmode with several different wavenumbers N_y (the same as that with $N_y = 0$ in Fig. 10) is presented in Fig. 11, from which we can see that the wider the range of values of the y component of the wave vector, the narrower the range of wavenumbers N_z where $\gamma > 0$ and the faster the instability growth rate.

An analysis of the general dispersion relation in the case of a nonzero electron velocity along the external magnetic field in the source region ($-l < x < l$) shows that the dependence of the growth rate of the cyclotron maser instability on N_z remains essentially unchanged as u_0 increases from 0 to 0.01. The results of relevant calculations for the $n = 12$ eigenmode are illustrated in Fig. 12 for the same plasma parameters as in Fig. 11. From the frequency dependence shown in Fig. 12, we can see that, for $u_0 \neq 0$, the real part of the frequency waves behave in such a way that, in the Earth's nonuniform magnetic field, the waves generated at $N_z = 0$ (or even at $N_z < 0$, which corresponds to the direction opposite to that of the magnetic field gradient, i.e., to the outward direction from the Earth) first propagate downward (because their group velocity is positive, $V_{gr} > 0$) until they reach the reflection point ($V_{gr} = 0$) and then they propagate upward to an altitude where their frequency becomes equal to the external local cutoff fre-

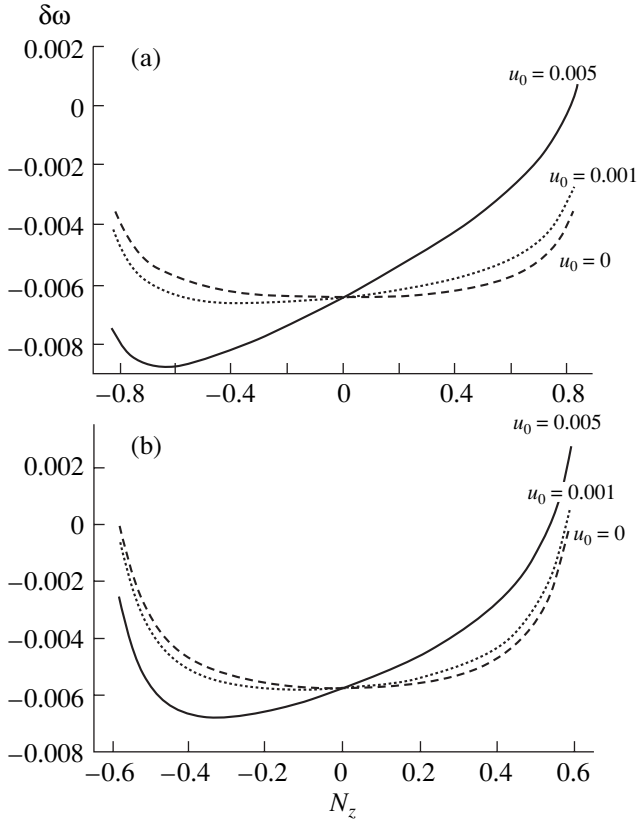

Fig. 12. Normalized wave frequency δω as a function of N_z for the $n = 12$ eigenmode with N_y = (a) 0 and (b) 0.7 at different values of u_0.

quency for an X mode. The external cutoff frequency in the region where the waves are generated is higher than the cutoff frequency in the source region because the plasma density outside the source is higher than that inside the source, but the cutoff frequency decreases with altitude because of the weakening of the magnetic field. Hence, even though the dependence of the growth rate on N_z does not change with u_0, the wave amplification coefficient in a nonuniform magnetic field can increase when $u_0 \neq 0$ because the waves remain in the generation region for a longer time.

4. CONCLUSIONS

We have constructed a waveguide model of the generation of electromagnetic waves that describes the development of electron maser instability in plasma regions of depressed density and finite length in one of the directions perpendicular to the magnetic field. Our investigation shows that the instability growth rates increase with increasing width of the generation region. For a certain width of the source region, the growth rates become as fast as those characteristic of a homogeneous plasma. For instance, for a source region with a width on the order of 60 km and for plasma parameters typical of the generation of AKR at a frequency on the order of 200 kHz, the linear instability growth rate is virtually the same as in a homogeneous plasma. The main effect of the finite length of the source region is that there is a preferential direction in which the fastest growing waves propagate. The numerical solution of the general dispersion relation derived in our model shows that the instability growth rate increases with the y component of the wave vector. We have constructed the eigenmodes of the waveguide and have shown that the electromagnetic field within the source region is generally asymmetric in structure. Symmetric solutions are possible only when the y component of the wave vector is zero. The polarization of the electromagnetic field of waves with a nonzero y component of the wave vector, $k_y \neq 0$, depends on the coordinates. The ratio of the absolute values of the electric field components, $|E_x|/|E_y|$, increases with k_y to maximum values on the order of several tens for waves with the maximum possible wave vector components k_y. Remember that it is the waves with the maximum values of k_y that grow at the fastest rates. Hence, it can be expected that the formation of the AKR spectrum should be dominated by waves propagating at the smallest angles to the y axis.

Our investigation of the dependence of the instability growth rates on the electron energy in the source region shows that, as the transverse electron energy increases, the growth rates become faster and the frequency range of the waves excited in the source broadens. The electron velocity component along the magnetic field is 0–0.01 of the speed of light and has essentially no effect on the instability growth rate. However, in a nonuniform magnetic field analogous to that of the Earth, the dependence of the real part of the frequency of the excited waves on the their wave vectors changes, with the result that the residence time of the waves within the source region can increase and, accordingly, their amplitudes can grow.

An analysis of the data from measurements done by the *Viking* [6] and *FAST* [12] satellites shows that AKR is emitted mainly along a tangent to the source boundary extended in a latitude direction. In this case, the wave polarization in a plane perpendicular to the magnetic field changes from nearly isotropic to highly anisotropic, dominated by the electric field component $|E_x|$, which is perpendicular to the AKR source boundary. In some cases, the ratio of the electric field components, $|E_x|/|E_y|$, can be as large as 100. These experimental data confirm that the waveguide model can adequately describe the generation of AKR. For a more detailed comparison of theoretical results with satellite observational data, we plan to carry out simulations of the amplification and propagation of electromagnetic waves with allowance for the Earth's nonuniform magnetic field.

ACKNOWLEDGMENTS

This work was supported in part by the Russian Foundation for Basic Research (project no. 05-02-17566), the RF Presidential Program for State Support of Leading Scientific Schools (project no. NSh-5359.2006.2), and the Joint Research Program with the French National Scientific Research Center (CNRS) (grant no. 19085).

REFERENCES

1. E. A. Benediktov, G. G. Getmantsev, N. A. Mityakov, et al., *Outer Space Investigation* (Nauka, Moscow, 1965) [in Russian].
2. D. A. Gurnett, J. Geophys. Res. **79**, 4227 (1974).
3. W. Calvert, J. Geophys. Res. **92**, 1267 (1987).
4. C. S. Wu and L. C. Lee, Astrophys. J. **23**, 621 (1979).
5. R. E. Ergun, C. W. Carlson, J. P. McFaden, et al., Astrophys. J. **538**, 456 (2000).
6. P. Louarn, Planet. Space Sci. **44**, 199 (1996).
7. P. Louarn, Planet. Space Sci. **44**, 211 (1996).
8. P. L. Pritchett, J. Geophys. Res. **89**, 8957 (1984).
9. R. J. Strageway, J. Geophys. Res. **91**, 3152 (1986).
10. D. Le Quéau and P. Louarn, J. Geophys. Res. **94**, 2605 (1989).
11. R. C. Davidson, in *Basic Plasma Physics*, Ed. by A. A. Galeev and R. N. Sudan (North-Holland, Amsterdam, 1984; Énergoatomizdat, Moscow, 1983). Vol. 1.
12. P. L. Pritchett, R. J. Strageway, R. E. Ergun, and C. W. Carlson, J. Geophys. Res. **107**, 1437 (2002).

Translated by O.E. Khadin